International Conference
Nuclear Energy for New Europe 2007
Portorož /Slovenia /September 10-13
port2007@ijs.si
www.nss.si/port2007
+386 1 588 5247, fax +386 1 588 5376
PORT2007, Nuclear Society of Slovenia, Jamova 39, SI-1000 Ljubljana, Slovenia

CFD Spray Simulations for Nuclear Reactor Safety Applications with Lagrangian Approach for Droplet Modelling

Miroslav Babić, Ivo Kljenak
Jožef Stefan Institute
Jamova ulica 39, SI-1000 Ljubljana, Slovenia
miroslav.babic@ijs.si, ivo.kljenak@ijs.si

ABSTRACT

The purposes of containment spray system operation during a severe accident in a light water reactor (LWR) nuclear power plant (NPP) are to depressurize the containment by steam condensation on spray droplets, to reduce the risk of hydrogen burning by mixing the containment atmosphere, and to collect radioactive aerosols from the containment atmosphere. While the depressurization may be predicted fairly well using lumped-parameter codes, the prediction of mixing and collection of aerosols requires a local description of transport phenomena.

In the present work, modelling of sprays on local instantenous scale is presented and the Design of Experiment (DOE) method is used to assess the influence of boundary conditions on the simulation results. Simulation results are compared to the TOSQAN 101 spray test, which was used for a benchmarking exercise in the European Severe accident research network of excellence (SARNET). The modelling approach is based on a Lagrangian description of the dispersed liquid phase (droplets), an Eulerian approach for the description of the continuous gas phase, and a two-way interaction between the phases. The simulations are performed using a combination of the computational fluid dynamics (CFD) code CFX4.4, which solves the gas transport equations, and of a newly proposed dedicated Lagrangian droplet-tracking code.

1 INTRODUCTION

Simulations of sprays with CFD codes have been done so far mostly in the automotive and chemical industries. Most polydispersed spray models have been based on either discretising the dispersed phase flow field into groups of equally sized droplets, as in the discrete droplet model (DDM) in which groups of droplets are tracked in space in a Lagrangian framework [1, 2], by solving separate Eulerian conservation equations for a number of size ranges [3], or by solving Eulerian transport equations for the statistical moments of droplet variables probability density functions [4]. All approaches can result in very long computational times, although the Lagrangian DDM approach is generally regarded as being superior in this respect under most conditions of interest [5].

Analyses of containment spray activation effects on the behaviour of steam and hydrogen in the Advanced Power Reactor (APR1400), European Pressurized Reactor (EPR) and current German nuclear power plants have been performed with the GASFLOW CFD code [6, 7, 8]. For the modelling of gas mixture and spray droplets flow, GASFLOW uses a homogenous two-phase flow model with assumption of thermal non-equilibrium and mechanical equilibrium between the phases. The analyses have shown that the use of sprays in loss-of-coolant accidents would generally reduce the risk of hydrogen burning in containment due to strong mixing of the atmosphere. The comparison of GASFLOW to lumped-parameter simulations have shown that lumped-parameter codes cannot conservatively predict the heterogenous local conditions during transition from stratified to well-mixed atmosphere [8].

In the present work, modelling of sprays on the local instantenous scale is presented. The modelling approach is based on a Lagrangian description of the dispersed liquid phase (droplets), an Eulerian approach for the description of the continuous gas phase, and a two-way interaction between the phases. The simulations are performed with a dedicated Lagrangian droplet-tracking code and the general-purpose computational fluid dynamics code (CFD) CFX version 4.4, which solves the gas transport equations.

The assessment of the sensitivity of simulation results to boundary conditions variation is performed using the Design of Experiment (DOE) method. This structured method is used to asses the relationship between parameters and results of spray simulations. In this work, the parameters of interest are the boundary conditions of the spray simulation. Their effect on equilibrium simulation results is assessed.

The simulation results are compared to experimental data, namely the TOSQAN 101 spray test, which was performed at the Institut de Radioprotection et de Surete Nucleaire (IRSN) in Saclay (France). The TOSQAN 101 spray test results were used for a spray benchmarking exercise performed in the European Severe accident research network of excellence (SARNET). In this test, a cold spray was injected into a 7 m^3 cylindrical vessel during 10000 s. The vessel was initially filled with hot air and steam, and vessel walls were kept at a sufficiently high temperature to prevent steam condensation. After initial depressurization, a steady state was reached, when the steam condensation on droplets was balanced by the evaporation of the liquid on hot walls.

2 TOSQAN 101 SPRAY TEST

The TOSQAN experimental facility is shown in Figure 1.a. It is a cylindrical vessel (7 m^3 volume, 4.8 m high, 1.5 m internal diameter) [9]. The temperature of the walls is controlled by heater oil circulation. The inner spray system, located in the dome of the vessel and centered on the vertical axis, is composed of a single nozzle producing a full cone water spray.

At the begining of the TOSQAN 101 spray test, the vessel is filled with air at 1 bar and 120 ^oC [10]. Then, superheated steam is injected into the vessel until a pressure of 2.5 bar is reached. After the steam injection is stopped, spraying starts on the vessel axis at 4.15 m elevation with a mass flow rate $\dot{m}_{inj}$ of 30 g/s. The initial water injection temperature T_{inj} of 130 ^oC reduces to equilibrium injection temperature of around 25 ^oC in approximately 200 s. The spray test can be divided into 4 phases [11, 12]:

- *Initial droplet evaporation phase* – The first 100 s after the start of spraying are characterized by a strong evaporation of droplets due to their high initial temperature (130 ^oC).

- *Condensation and mixing phase* – The next 200 s are characterized by the transition to

the atmosphere saturation state which was driven by steam condensation on droplets and cooling by convective heat transfer to droplets.

- *Condensation phase* – Slow decrease of gas temperature and steam mass during the next 3000 s.

- *Equilibrium phase* – During this phase, the heat supplied by the vessel walls is equal to the heat extracted from the gas by the droplets, which is required to bring droplets from injection temperature to steam saturation temperature.

Both intrusive and non-intrusive measuring techniques are implemented in the experimental facility [9]. Velocities are measured with particle image (PIV) and laser Doppler (LDV) velocimetry with accuracies ranging from $1-5\%$ and $2-10\%$, respectively. Gas concentrations are measured with a mass sprectrometer and spontaneous Raman scattering spectroscopy (SRS) with accuracy of $\pm$ 1.5 vol. % and $\pm$ 1 vol. %. Gas temperatures are measured with thermocouples with accuracies of $\pm$ 1 ^oC. The interferometrics laser imaging for droplets sizing (ILIDS) is used for measuring spray droplets size distribution with accuracy of 5 %.

3 SIMULATION PROCEDURE

3.1 Continuous phase solver

For the solution of the gas transport equations, the CFD code CFX4.4 is used. The discretisation of the equations in the CFX code is based on a conservative finite-volume method. The code has been already successfuly used for the simulation of containment phenomena [13, 14, 15].

The atmosphere in the TOSQAN facility is modelled as a single-phase gaseous mixture that is homogeneous within each computational cell, with air as the "carrier fluid". The flow is modelled as compressible and buoyant. Turbulence is modelled with a standard $k-\epsilon$ model, with the $C_{3\epsilon}$ constant set to 1.

A two-dimensional axisymmetric model (in cylindrical coordinates) for the code CFX4.4 is used. The computational domain is a block with 50 cells in the axial (vertical) direction and 12 cells in the radial (horizontal) direction (Fig. 1.b). There are 600 cells altogether. Cell widths (radial direction) in the spray-affected gas region are smaller than cell widths near the vessel walls.

3.2 Dispersed phase solver

The simulation of the dispersed phase behaviour is achieved by integration of droplet transport equations in a Lagrangian framework. The procedure is composed of 3 major steps, which are explained below:

- Creation of new droplet groups at the spray injection location.

- Calculation of droplets-to-gas momentum, heat and mass transfer.

- Calculation of heat and mass transfer from the liquid on the walls to the gas.

Creation of new droplet groups. Each droplet group represents a group of droplets possessing equal characteristics such as position, velocity, size and temperature. For each Lagrangian step with a timestep size of Δt_D, K_{gr} groups are created with equal mass $m_{group} = \dot{m}_{inj} \cdot \Delta t_D / K_{gr}$. Their temperature is equal to the injection temperature T_{inj}. The size of

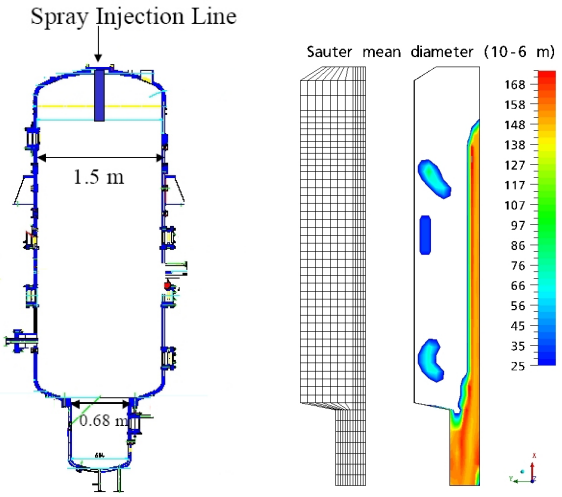

(a) TOSQAN vessel.

(b) Numerical mesh (left) and calculated spray mean Sauter diameter field (right).

Figure 1: TOSQAN vessel and numerical mesh.

droplets in the group is determined by randomly selecting a droplet diameter D from a normal distribution with mean D_{ave} and variance σ_D^2. From this, the number of droplets in each group can be determined. Each group is assigned an injection speed U_{inj}. The initial radial position of a droplet is $r = (1 - U^2)R_{inj}$, where U is a uniform random number in the interval $(0, 1)$ and R_{inj} is the half-width of the spray. This starting position and the nozzle location are used to determine the angle of droplet injection and thus the velocity components.

Droplets to gas momentum, heat and mass transfer. The dispersed phase is considered to be in the form of discrete single-component spherical liquid droplets. Momentum transfer between phases is only a function of the drag force, and thermal energy exchange between phases is assumed only to occur through convective heat transfer. In the present version of the model, droplet-to-droplet interactions and effects of spray on turbulence are neglected. Under this assumptions, we can write the generic Lagrangian equations describing the transient position (X_i), velocity (v_i), temperature (T_d) and mass (m_d) of a single droplet representing a particular group ([16]):

$$\frac{\mathrm{d}X_i}{\mathrm{d}t} = v_i, \tag{1}$$

$$\frac{\mathrm{d}v_i}{\mathrm{d}t} = \frac{f_1}{\tau_d}(u_i - v_i) + g_i, \tag{2}$$

$$\frac{\mathrm{d}T_d}{\mathrm{d}t} = \frac{Nu_d}{3Pr_G}\left(\frac{\theta_1}{\tau_d}\right)(T_G - T_d) + \frac{L_V}{C_L}\frac{\dot{m}_d}{m_d}, \tag{3}$$

$$\frac{\mathrm{d}m_d}{\mathrm{d}t} = -\frac{Sh_d}{3Sc_G}\left(\frac{m_d}{\tau_d}\right)H_M, \tag{4}$$

where the subscripts denote vector component i, droplet d, gas phase property away from droplet surface G, vapor phase V of the evaporate, and liquid L. The variation of droplet mass $\dot{m}_d = \mathrm{d}m_d/\mathrm{d}t$ is negative for evaporation, u_i and T_G are the local carrier gas velocity

and temperature, g_i is the gravitational acceleration, L_V is the latent heat of evaporation, and θ_1 is the ratio of the gas (constant pressure) to liquid heat capacity. The gas phase Prandtl and Schmidt numbers in terms of the viscosity μ, thermal conductivity λ, diffusion coefficient Γ are $Pr_G = \mu_g C_{p,G}/\lambda_G$ and $Sc_G = \mu_G/(\rho_G \Gamma_G)$. The particle Nusselt number Nu_d and particle Sherwood number Sh_d are calculated with widely used Ranz and Marshall correlations.

$$Nu_d = 2 + 0.552 Re_d^{1/2} Pr_G^{1/3}, \quad Sh_d = 2 + 0.552 Re_d^{1/2} Sc_G^{1/3}. \tag{5}$$

In equations (2)-(4), $\tau_d = \rho_d D^2/(18\mu_G)$ is a particle time constant for Stokes flow and f_1 is a correction to Stokes drag due to evaporation:

$$\begin{aligned} f_1 &= \frac{1}{1 + a|Re_b|^b} \cdot \left[0.0545 Re_d + 0.1 Re_d^{1/2}(1 - 0.03 Re_d) + 1 \right], \\ a &= 0.09 + 0.077 \exp(-0.4 Re_d), \quad b = 0.4 + 0.77 \exp(-0.04 Re_d), \end{aligned} \tag{6}$$

where $Re_d = \rho_G u_s D/\mu_G$ is the particle Reynolds number, based on slip velocity $u_s = |u_i - v_i|$, and $Re_b = \rho_G u_b D/\mu_G$ is the Reynolds number, based on blowing velocity $\dot{m}_d = -\pi \rho_G D^2 u_b$. $H_M = (Y_d - Y_g)/(1 - Y_d)$ represents the specific driving potential for mass transfer between gas and droplet surface. The gas and vapor properties are evaluated at the reference temperature T_R and steam mass fraction Y, which are calculated using the so-called $A = 1/3$ rule ($T_R = T_d + A(T_G - T_d)$, $Y_R = Y_d + A(Y_G - Y_d)$).

The numerical solution of this part follows the idea of Dukowicz [17], where, instead of a simultaneous solution of equations (1)-(4), the splitting technique is used. In the first part, the droplets momentum equations (1)-(2) are solved with the assumption that droplet temperatures, masses and gas velocity do not change. In the second part, the enthalpy and vapor mass fraction source terms are calculated by solving energy and mass conservation equations of all droplets and gas in control volume simultaneously and treating the control volume as a closed system [18]. Droplets to gas heat and mass transfer is calculated using equations (3)-(4) by taking average droplet velocity from the previous step.

Liquid on walls heat and mass transfer. When droplet groups reach the wall, they are treated as a stationary liquid film on faces of wall computational cells. The assumption that the liquid on the walls does not move seems reasonable, since only a small fraction of droplets reaches walls other than the vessel bottom. Those groups that reach the vessel bottom are collected to form a water pool in the sump. The rest of droplets that reach "dry" walls quickly evaporate. For the liquid film to gas heat and mass transfer, the same approach is taken as for the droplets to gas transfers and the following equations are used:

$$\dot{T}_F = (Q_{wall} + Q_{conv} + \dot{m}_F L_V)/(m_F \cdot c_F), \quad \dot{m}_F = -h_M \cdot A_F \cdot M_s \cdot \frac{x_F - x_G}{1 - x_F}, \tag{7}$$

where x_G and x_F denote the steam volume fraction in the gas and the saturation steam volume fraction at liquid film temperature, c_F is the liquid heat capacity, A_F is the film covered wall surface, M_s is the steam molar weight, $Q_{conv} = Nu_F \cdot \lambda_G \cdot A_F \cdot (T_G - T_F)/L$ is the liquid-to-gas heat transfer rate and the film Nusselt number Nu_F is calculated with a forced turbulent convection correlation [19]:

$$Nu_F = 0.029 Re_L^{0.8} Pr_G / \left[\sqrt{\frac{0.029}{Re_L^{0.2}}} (5Pr + 5\ln((1 + 5Pr)/6) - 5) + 1 \right], \tag{8}$$

where the Reynolds number $Re_L = |u_i| L/\nu_G$ is based on the length of the wall computational cell L. The mass transfer coefficient h_M is calculated from Nu_F using Chilton-Colburn analogy.

$Q_{wall} = Nu_w \cdot \lambda_L \cdot A_F \cdot (T_W - T_F)/\delta_F$ is the wall-to-liquid heat transfer rate, where δ_F is the liquid film thickness. Wall to liquid heat transfer Nusselt number is calculated using the following equation:

$$\begin{aligned} Nu_w &= \max\left[2\ ;\ 0.06765 \cdot Ra_{\delta_F}^{0.309}\right], \\ \text{with } Ra_{\delta_F} &= g\beta|T_W - T_F|\delta_F^3 c_L \rho_L/(\nu_L \lambda_L), \end{aligned} \tag{9}$$

where the constant expression in Eq. 9 refers to wall to liquid heat transfer with conduction in case of very thin liquid film on the so-called dry walls and the r.h.s. is a convective wall-to-liquid heat transfer coefficient correlation based on Rayleigh number Ra in case of liquid pool formation in the vessel sump.

4 SENSITIVITY ANALYSIS

The assessment of the sensitivity of simulation results to boundary conditions variation is performed using the Design of Experiment (DOE) method. This structured method is used to assess the relationship between parameters affecting the spray simulation results. A similar sensitivity analysis was performed for the TONUS CFD code applied to containment hydrogen burning risk analyses [20]. In this work, we adopt the so-called "Screening Design", since only first-order interactions are of interest. Thus, a Linear Response Model (LRM) without interactions is selected. In this model, $M + 1$ regression coefficients a_j need to be determined for each selected response variable Y and M parameters X_j:

$$Y = a_0 + \sum_{j=1}^{M} a_j \cdot X_j\ . \tag{10}$$

When parameters are normalized and can have only two values ± 1, at least $M + 1$ simulation runs are needed to determine the coefficients a_j. The proper parameter variation is given by a matrix of parameters $A_{i,j}$, where row i of the matrix contains the values of parameters in single experiment / simulation. Plackett and Burman proposed that an efficient choice for this task is the Hadamard square matrix H of order $M + 1$ [21]. The coefficients of the Hadamard matrix have values ± 1 and following relationship holds $H \times H^T = (M + 1)I$, where I is the unit matrix.

$$H_{i,j} = \begin{pmatrix} 1 & 1 & -1 & -1 & 1 & -1 & 1 & 1 \\ 1 & 1 & 1 & -1 & -1 & 1 & -1 & 1 \\ 1 & 1 & 1 & 1 & -1 & -1 & 1 & -1 \\ 1 & -1 & 1 & 1 & 1 & -1 & -1 & 1 \\ 1 & 1 & -1 & 1 & 1 & 1 & -1 & -1 \\ 1 & -1 & 1 & -1 & 1 & 1 & 1 & -1 \\ 1 & -1 & -1 & 1 & -1 & 1 & 1 & 1 \\ 1 & -1 & -1 & -1 & -1 & -1 & -1 & -1 \end{pmatrix} \tag{11}$$

The parameters of interest are the boundary conditions of the spray simulation: injection speed of droplets U_{inj}, spray angle ϕ_{spray}, average droplet diameter D_{ave} and standard deviation σ_D of the volumetric droplet distribution, spray injection temperature T_{inj} and wall temperature T_{wall}. Table 1 gives the reference values of selected parameters and their variation used for the DOE analysis.

Table 1: Parameters with their reference values and their magnitude of variation (*: prescribed time-dependent variation).

Parameter	U_{inj}	$\phi_{spray}/2$	D_{ave}	σ_D^2	T_{inj}	T_{wall}
Unit	m/s	^{o}	μm	μm	^oC	^oC
Reference value	10	28.5	150	500	*	*
Change	$\pm$ 1	$\pm$ 1.5	$\pm$ 5	$\pm$ 50	$\pm$ 1	$\pm$ 0.5

5 RESULTS

5.1 Simulation with reference values of parameters

In this section, the results of simulation with reference values of parameters are presented. The simulation-experiment comparisons of total pressure and average atmosphere temperature are shown in Figure 2. The simulation results agree quite well with the experimental data.

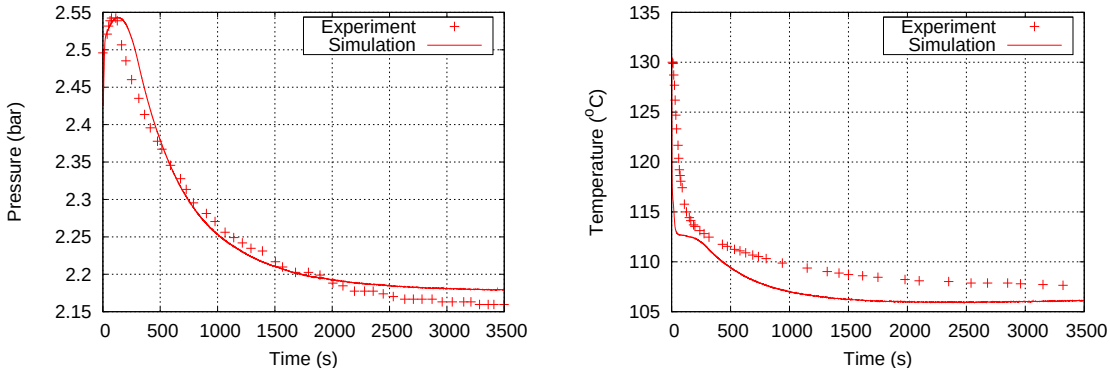

(a) Pressure. (b) Average atmosphere temperature.

Figure 2: Comparison of calculated and measured integral data.

The simulation-experiment comparison of droplet velocities at equilibrium is shown in Figure 3. The vertical velocity on the vessel axis is underpredicted (Fig. 3.a) near the injection location, while the agreement improves away from the injection nozzle. For the radial profile of droplet vertical velocity 450 mm below the injection location (Fig. 3.b), the predicted profile exhibits step changes in velocity values. Each step change indicates the boundary of gas solver computational cell. This is due to the assumption that there are no gradients of gas velocities inside computational cells.

Figure 4 shows vertical profiles of steam volume fraction on the vessel axis below the injection location at equilibrium. The calculated steam content evolution in Fig. 4.a shows three distinct regions in the vessel:

- *just bellow the injection location*, from 0 m to 1 m away from the nozzle, where the steam content is reduced due to condensation on cold droplets,
- *in the sump* (from 3.0 m away from the nozzle), where the steam content increases due to evaporation from the water pool and dry vessel walls, and
- *intermediate region*, where the steam content gradually increases due to steam evaporation from gas-heated droplets.

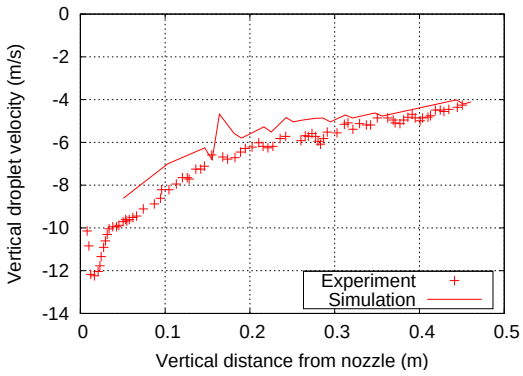

(a) Measured and calculated vertical profiles of droplet velocity on vessel axis.

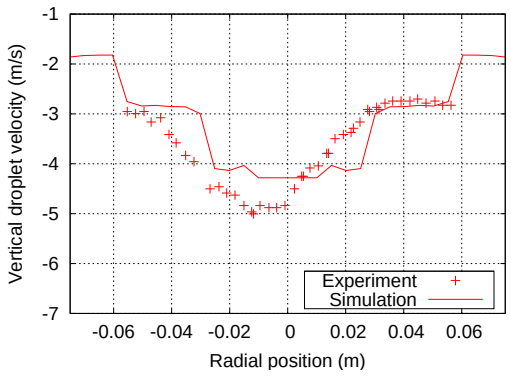

(b) Measured and calculated radial profiles of droplet velocity 450 mm below nozzle.

Figure 3: Comparison of calculated and measured profiles of droplet vertical velocity component at equilibrium.

In Fig. 4.b, it can be observed that the simulation correctly predicts a gradual increase of steam volume fraction moving away from the spray nozzle, but significantly overpredicts the steam content in the region below the injection location. However, the dispersion of experimental results is an indication of their uncertainty.

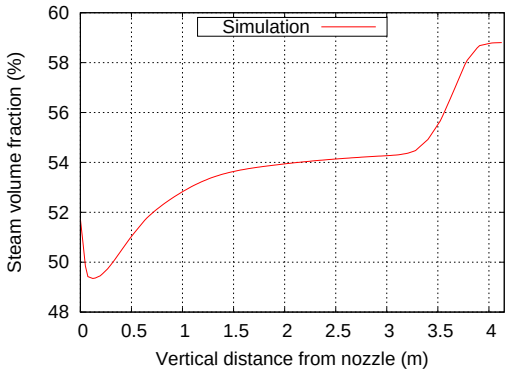

(a) Entire vessel.

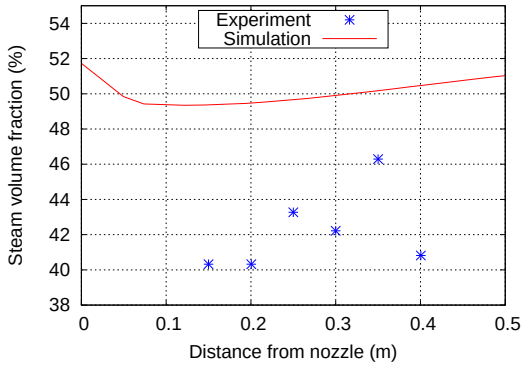

(b) Below nozzle.

Figure 4: Measured and calculated vertical profiles of steam volume fraction on vessel axis at equilibrium.

Figure 5 compares measured and calculated radial profiles of gas temperatures at 3.93 m and 1.47 m vessel elevation at equilibrium. Calculated profiles agree qualitatively well with the experimental results. Measured and calculated profiles at the 3.93 m elevation show that temperatures decrease near the vessel axis due to strong liquid-to-gas heat and mass transfer. The calculated profile is narrower and temperature values on the vessel axis are somewhat lower than in the experiment (Fig. 5.a).

Figure 6 shows measured and calculated droplet diameter distributions at 1260 s on the vessel axis at 2.8 m elevation. Measured and calculated mean droplet diameters $D_{10} = \sum_i n_i d_i / \sum_i n_i$ are similar (146 and 133 μm), but there is a considerable difference between measured and calculated Sauter mean diameter $D_{32} = \sum_i n_i d_i^3 / \sum_i n_i d_i^2$ (198 and 144 μm) since the simulation

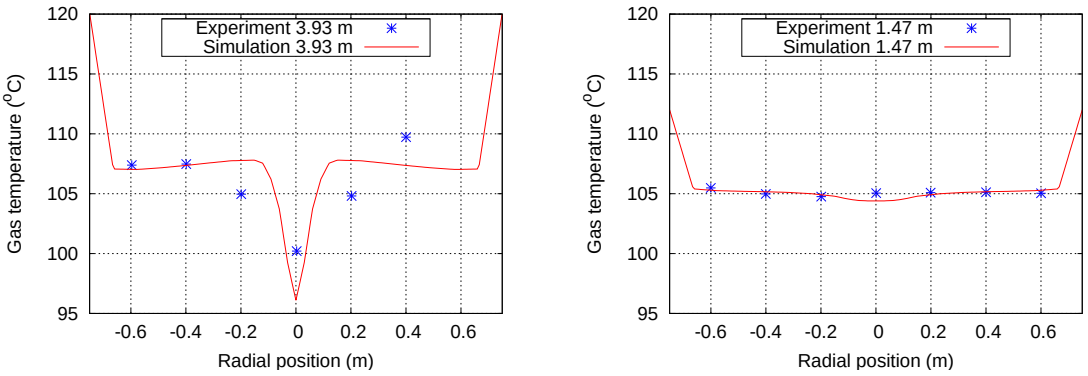

(a) 3.93 m elevation. (b) 1.47 m elevation.

Figure 5: Measured and calculated radial profiles of gas temperature at equilibrium.

has virtually no droplets with diameters above 200 μm due to the shape of the assumed initial droplet diameter distribution.

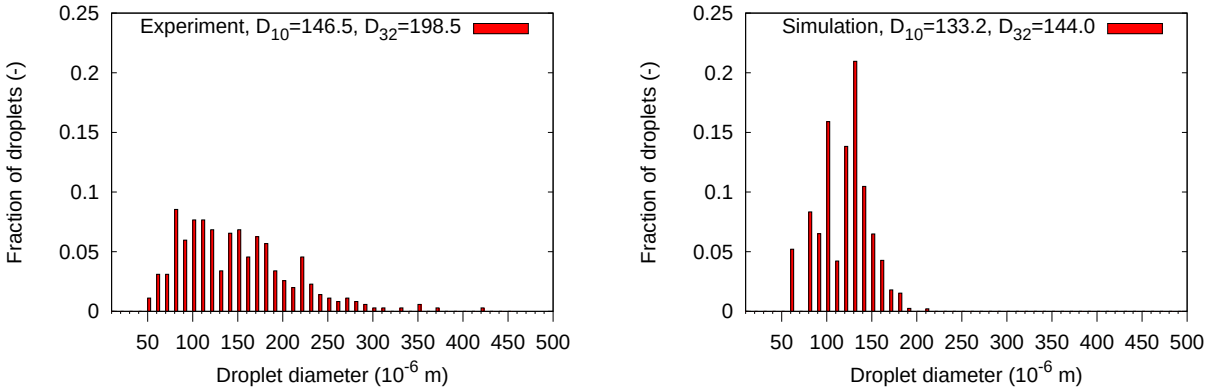

(a) Experiment. (b) Simulation.

Figure 6: Measured and calculated droplet diameter distribution at 1260 s.

5.2 Steady state sensitivity study

In this section, a steady-state sensitivity study of boundary conditions on simulation results is presented. For the simulation responses, the total pressure P_{tot}, the average containment atmosphere temperature T_{ave}, the droplet-to-gas $\dot{m}_{d\rightarrow g}$ and the liquid on all walls (including sump) to gas $\dot{m}_{w\rightarrow g}$ mass transfer rates, and the droplet-to-gas $\dot{Q}_{d\rightarrow g}$ convective heat transfer rate are selected. The regression coefficients of the linear response model (LRM) for the above-mentioned responses are shown in Table 2. The sign of a regression coefficient determines how the response changes when the parameter is increased.

For all selected responses, the injection speed U_{inj} is the dominant parameter with the largest LRM regression coefficient. The average diameter D_{ave} and the variance of droplet volume distribution σ_D^2 are the second most important parameters. An increase of injection speed and of average diameter affects the amount of steam in the vessel by increasing the particle Reynolds

Table 2: Results of steady state sensitivity study.

		P_{ave}	T_{ave}	$\dot{m}_{d\to g}$	$\dot{m}_{w\to g}$	$\dot{Q}_{d\to g}$
		bar	^oC	g/s	g/s	W
Reference calc.	R	2.16	106.43	0.00	0.00	-1760.93
LRM prediction	R_{LRM}	2.11	105.23	0.00	0.00	-1963.11
Relative difference	$\frac{R-R_{LRM}}{R}\cdot 100\%$	-2.51	-1.13	-6.32	-8.55	11.48
Regression coefficients $a_j^* = a_j/a_0 \cdot 100\%$						
a_1^*	U_{inj}	3.7	1.4	6.7	8.4	-12.1
a_2^*	$\phi_{spray}/2$	0.6	0.2	1.4	3.7	-1.2
a_3^*	D_{ave}	-0.7	-0.3	3.9	3.4	2.9
a_4^*	σ_D^2	2.1	0.8	3.1	5.2	-8.0
a_5^*	T_{inj}	0.4	0.2	-0.8	-1.1	-1.6
a_6^*	T_{wall}	1.2	0.5	1.3	1.2	-1.7

number Re_d and thus increasing the droplets-to-gas heat and mass transfer coefficients. Similarly, an increase in variance of the droplet volume distribution increases the total droplets surface area.

5.3 Analysis

The simulation of the TOSQAN 101 spray test on a relatively coarse mesh of 600 computational cells on a single 3 GHz Pentium-IV processor with 512 Mb RAM lasted about 300 h. The time-step size used for the CFD gas solver was 0.03 s.

Although the calculated pressure and the average containment atmosphere temperature agree quite well with the experimental data, the comparison of local variables reveals certain discrepancies. Increasing the injection speed and the mesh resolution in the radial direction in the spray-affected region should improve the agreement of calculated vertical and radial velocity profiles (Fig. 3.b), although this would significantly increase the computational time. The overprediction of steam volume fractions (Fig. 4.b) and the underpredicted temperature (Fig. 5.b) on the vessel axis below the injection location could be attributed to deficiencies of simplified spray-gas momentum exchange and turbulence modelling:

- It is well known that the standard $k-\epsilon$ model overpredicts the turbulent diffusivity in high shear stress areas that occur on the border of spray-affected gas regions.
- The spray volume fraction of up to $6\cdot 10^{-4}$ suggests that turbulence modulation by sprays should be taken into account [22].

The underpredicted Sauter mean diameter causes perhaps higher gas entrainment by spray below the nozzle and stronger gas recirculation adjacent to injection location. This, coupled with defficiencies of spray-gas momentum exchange description, results perhaps in different spray characteristics compared to experiment. This is indicated in the steady-state sensitivity analysis, where the injection speed and the parameters of the volumetric droplet distribution affect the selected responses most. Thus, special attention to specification of these boundary conditions is required when local predictions are the goal of spray simulations.

6 CONCLUSIONS

A simulation method based on a combination of a Lagrangian approach for droplet-tracking and the general purpose CFD code CFX4.4 for the continuous phase was developed for spray simulation. The code was used to simulate the TOSQAN 101 air-steam spray test, which was performed at the Institut de Radioprotection et de Surete Nucleaire (IRSN), France. A two-dimensional axisymmetric model for the code CFX4.4 was developed, and spray-gas interaction was modelled with sinks of momentum, heat and mass, calculated with the newly proposed Lagrangian droplet-tracking code.

Calculated data, that is droplet velocities, gas temperatures, steam concentrations and droplet size distributions were compared to experimental measurements. Although the grid quality was limited by long computational times and simplified spray-gas momentum exchange and turbulence modelling were used, the simulation results agree reasonably well with the measured data and adequately reproduce the non-homogenous structure of the gas atmosphere. The boundary condition sensitivity study has shown that the most important factors affecting simulation results are injection speed and parameters of droplet size distribution.

Despite some discrepancies, the general agreement between experimental and calculated results shows that the proposed approach is adequate and that it could be, with further improvements, applied to similar problems.

ACKNOWLEDGMENTS

The research presented in the present work was performed within the research project J2-6614 (contract no. 3311-04-8226614) financed by the Ministry of Higher Education, Science and Technology of the Republic of Slovenia.

The Jožef Stefan Institute is a member of the Severe Accident Research Network of Excellence (SARNET) within the 6th EU Framework Programme. The benefit from European Commission RTD Programme for research is acknowledged.

REFERENCES

[1] S.S. Yoon, J.C. Hewson, P.E. DesJardin, D.J. Glaze, A.R. Black and R.R. Skaggs. Numerical modelling and experimental measurements of a high speed solid-cone water spray for use in fire suppresion applications. *International Journal of Multiphase Flow*, 30:1369-1388, 2004.

[2] D. Ducret, Y. Billarand, D. Roblot and J. Vendel. Study on collection efficiency of fission products by spray: experimental device and modelling. In *Proceedings of* 24^{th} *DOE / NRC Nuclear Air and Treatment Conference*, Portland, Oregon, 1996.

[3] F. Laurent, M. Massot and P. Villedieu. Eulerian multi-fluid modelling for the numerical simulation of coalescence in polydisperse dense liquid sprays. *Journal of Computational Physics*, 194:505-543, 2004.

[4] J.C. Beck, and A.P. Watkins. On the development of spray submodels based on droplet size moments. *Journal of Computational Physics*, 182:586-621, 2002.

[5] J.C. Beck, and A.P. Watkins. The droplet number moments approach to spray modelling: The development of heat and mass transfer sub-models. *International Journal of Heat and Mass Transfer*, 24:242-259, 2002.

[6] J. Kim, U. Lee, S.W. Hong, S.B. Kim and H.D. Kim. Spray effect on the behaviour of hydrogen during severe accidents by a loss of coolant accidents in the APR1400 containment. *International Communications on Heat and Mass transfer*, 33:1207-1216, 2006.

[7] M.A. Movahed, J. Eyink and J.R. Travis. Effect of spray activation on the reactivity of the hydrogen-air-steam mixture in the containment of the European pressurized water reactor (EPR). In *Proceedings of* 10^{th} *International Topical Meeting on Nuclear Reactor Thermal Hydraulics (NURETH-10)* , Seoul, Korea, 2003.

[8] P. Royl, H. Rochholz, W. Breitung, J.R. Travis and G. Necker. Analysis of steam and hydrogen distributions with PAR mitigation in NPP containments. *Nuclear Engineering & Design*, 202:231-248, 2000.

[9] E. Porcheron, P. Lemaitre, A. Nuboer, V. Rochas and J. Vendel. Experimental investigation in the TOSQAN facility of heat and mass transfers in a spray for containment applications. *Nuclear Engineering & Design*, 237:1862-1871, 2007.

[10] J. Malet, E. Porcheron, J. Vendel, L. Blumenfeld and I. Tkatschenko. Sarnet Spray Benchmark: TOSQAN and MISTRA - Specification report - Revision 1. *Rapport DSU/SERAC/LEMAX/06-11*, May 2006.

[11] P. Lemaitre, A. Nuboer, and E. Porcheron. Analysis of Spray Test No. 101. *Rapport DSU/SERAC/LEMAX/07-02*, January 2007.

[12] P. Lemaitre, A. Nuboer and E. Porcheron. TOSQAN Experimental Report – Spray Test 101. DSU / SERAC / LECEV / 05–11, Institut de Radioprotection et de Surete Nucleaire, Saclay, France, 2005.

[13] M. Houkema, N.B. Siccama, J.A .Lycklama $\grave{a}$ Nijeholt and E.M.J. Komen. Validation of the CFX4 CFD code for containment thermal-hydraulics. *Nuclear Engineering & Design*, (doi:10.1016/j.nucengdes.2007.02.033), 2007.

[14] M. Babić, I. Kljenak and B. Mavko. Prediction of light gas distribution in experimental containment facilities using the CFX4 code. *Nuclear Engineering & Design*, (doi:10.1016/j.nucengdes.2007.02.039), 2007.

[15] I. Kljenak, M. Babić, B. Mavko and I. Bajsić. Modeling of containment atmosphere mixing and stratification experiment using a CFD approach. *Nuclear Engineering & Design*, 236:1682-1692, 2006.

[16] R.S. Miller, K. Harstad, J. Belan. Evaluation of equilibrium and non-equilbrium evaporation models for many-droplet gas-liquid flow. *International Journal of Multiphase Flow*, 24:1025-1055, 1998.

[17] J.K. Dukowicz. A particle-fluid numerical model for liquid spray. *Journal of Computational Physics*, 35:229-253, 1980.

[18] P.I. Aguayo, C. Weiß. Enthalpy two way coupling for near vapor saturated polydispersed spray flows. In *Proceedings of* 5^{th} *International Conference on Multiphase Flows, ICMF'04*, Yokohama, 2004.

[19] A. Bejan and A.D. Kraus. *Heat transfer handbook*. John Wiley & Sons, Inc., New York, 2003.

[20] S. Kudriakov, F. Dabbene, E. Studer, A. Beccantini, J.P. Magnaud, H. Paillere, A. Bentaib, A. Bleyer, J. Malet, E. Porcheron and C. Caroli. The TONUS CFD code for hydrogen risk analysis: Physical models, numerical schemes and validation matrix. *Nuclear Engineering & Design*,(doi:10.1016/j.nucengdes.2007.02.048), 2007.

[21] C. Croarkin and P. Tobias ed. Handbook of Statistical Methods. *NIST/SEMATECH e-Handbook of Statistical Methods, http://www.itl.nist.gov/div898/handbook/*, 16. 7. 2007.

[22] W.A. Sirignano. *Fluid dynamics and transport of droplets and sprays*. Cambridge University Press, Cambridge, 2000.